IDENTIFICATION OF FRICTION ENERGY DISSIPATION USING FREE VIBRATION VELOCITY: MEASUREMENT AND MODELING

Christoph A. Kossack, Tony L. Schmitz, and John C. Ziegert
Department of Mechanical Engineering and Engineering Science
University of North Carolina at Charlotte
Charlotte, NC

INTRODUCTION

Existing force-based methods for parametrizing friction models are limited by large uncertainties (approximately parts in 10^2 [1]). This paper provides experimental results for a new method that uses velocity measured during free vibration to quantify the energy dissipation in friction contacts. The final goal is a friction measurement method that provides reduced uncertainty, particularly for low friction and low velocity applications.

FRICTION MEASURING MACHINE

The friction measuring machine (FMM) was designed and constructed to provide relative (linear) motion between the pin and counterface in a friction contact using a parallelogram leaf-type flexure [2]. The FMM can therefore be represented by a single degree of freedom spring-mass-damper system.

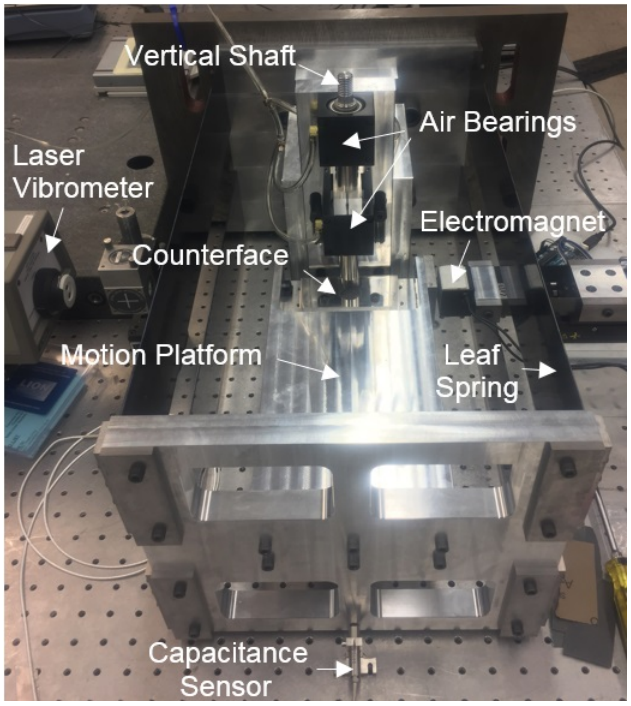

Figure 1. FMM photograph.

As shown in Fig. 1, the FMM uses four leaf springs to provide horizontal oscillating motion of the counterface. The FMM structure is based on a linear flexure mechanism. One end of each leaf spring is clamped to a rigid base, while the other is clamped to the faceplate that is attached to the motion platform. An electromagnet is used to capture the motion platform and displace it from its equilibrium position to provide the desired initial displacement. The force being applied by the electromagnet mechanism is located at the midpoint of the length of the flexures. This ensures that the faceplate will move parallel to the base plate, which, in turn, minimizes the rotation of the motion platform during friction testing.

A counterface is attached to the motion platform. The fixed pin is attached to the bottom of a vertical shaft which provides the dead weight normal force during friction tests. The shaft is held in place using two air bearings that are rigidly attached to the FMM base.

The gravitational load provides a constant normal force for the friction tests. The friction contact is completed when the pin is lowered onto the interchangeable translating counterface. The electromagnet is then used to move the motion platform to the desired initial displacement. Once the electromagnet is released, the system oscillates freely until it comes to rest.

The magnitude of the flexure's parasitic motion at the motion platform was estimated using Eq. 1 [2].

$$\Delta y = \frac{-3\Delta x^2}{5L} \tag{1}$$

Calculations show that the velocity measured with the laser vibrometer is two orders of magnitude larger than the parasitic motion for the range of tested displacements. To validate the calculations, a pair of capacitance sensors were used to measure the parasitic displacement of the motion platform and the results confirmed the analytical solution given by Eq. 1. Due to the small motion amplitude, the kinetic energy associated with the parasitic motion was neglected.

Free vibration velocity with no friction contact was measured to determine the instrument's dynamic characteristics, including the modal mass, *m*, stiffness, *k*, and viscous damping coefficient, *c*. A range of initial displacements was tested and a

nonlinear least-squares fitting algorithm was applied to Eq. 2 to determine the modal parameters [3].

$$m\ddot{x} + c\dot{x} + kx = 0 \quad (2)$$

CHARACTERIZATION OF SYSTEM DYNAMICS

The maximum allowable deflection for the FMM was calculated using Eq. 3:

$$\delta_{max} = \frac{\sigma_y L}{3Et}, \quad (3)$$

where *L* and *t* are the length and thickness of the leaf springs, respectively, and σ_y and *E* are the yield strength and elastic modulus for the spring material, respectively. The resulting maximum allowable deflection is 132 mm. A factor of safety of six was used to ensure that there would be no plastic deformation of the leaf springs. As a result the maximum testing displacement was 22 mm.

Free vibration, non-friction tests were performed with initial displacements ranging from {4 to 22} millimeters. For each test, the FMM was first moved to an initial displacement. The vibrometer was then initiated to begin collecting data. The motion platform was then released and allowed to oscillate freely for 45 s. The electromagnet was retracted upon release of the platform. For the flexure's natural frequency of 2.2 Hz, approximately 100 cycles were completed during the measurement interval.

Before the fitting algorithm was applied to the data set, the pre-slide velocity data was used to remove any initially velocity offset from zero and then a smoothing function was applied to the data. The first 10 cycles of the data set were also removed to ensure there were no residual effects from the electromagnet's release and charge dissipation. The fitting algorithm was then applied to the remaining data.

Equation 2 was the governing equation of motion for the system. Euler Integration was used in the fitting function to determine the modal parameters. The fitting algorithm was the Matlab® nonlinear least squares fitting algorithm *lsqnonlin*, which implements a trust region reflective fitting approach. Figure 2 displays a sample of the fitting results using this function and Fig. 3 shows a small section of Fig. 2 to better illustrate the fitting results.

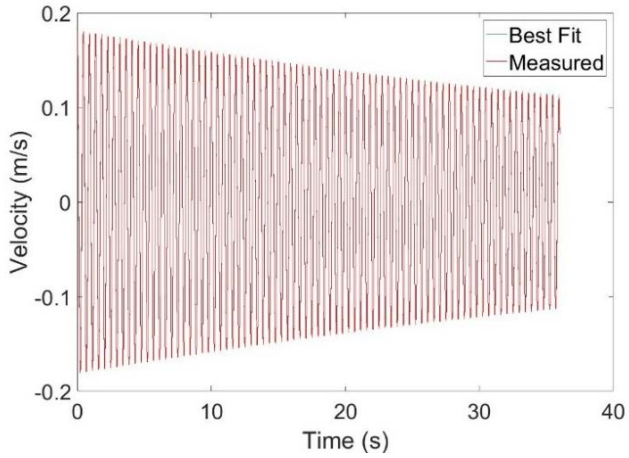

Figure 2. Velocity data fitting results.

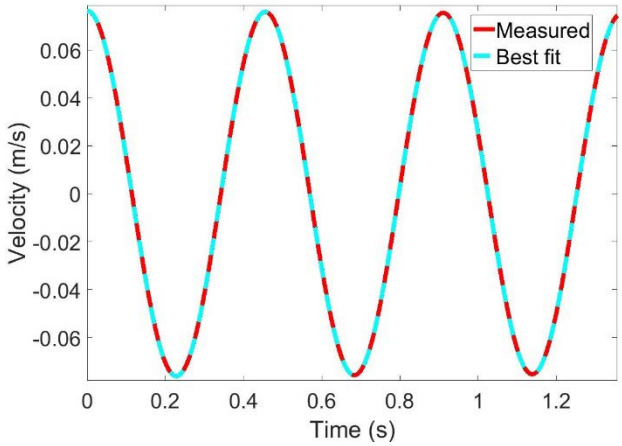

Figure 3. Section of velocity data fitting results.

The modal parameters identified using the fitting routine for various initial displacements are displayed in Table 1 and the mean values and standard deviations are presented in Table 2.

Table 1. Modal parameters from fitting results.

Initial Displacement (mm)	Peak Velocity (mm/s)	Mass (kg)	Stiffness (N/m)	Viscous Damping (Ns/m)
4	50	10.394	1981	0.222
6	76	10.395	1981	0.235
8	103	10.393	1981	0.245
10	129	10.397	1982	0.256
14	181	10.392	1982	0.278
16	207	10.389	1983	0.288
18	233	10.389	1984	0.299
20	258	10.385	1984	0.313
22	283	10.382	1984	0.327

Table 2. Mean and standard deviation of modal parameters.

Modal Parameters	m (kg)	k (N/m)	c (Ns/m)
Mean	10.391	1982	0.275
St. Deviation	0.0045	1.3	0.0341

The damping coefficient showed the highest variation. Upon further inspection it was discovered that there appears to be a direct relationship between the viscous damping coefficient and the initial displacement, and, therefore the peak velocity during the free vibration cycle. This relationship is presented in Fig. 4. The linear fit has an R^2 value of 0.997.

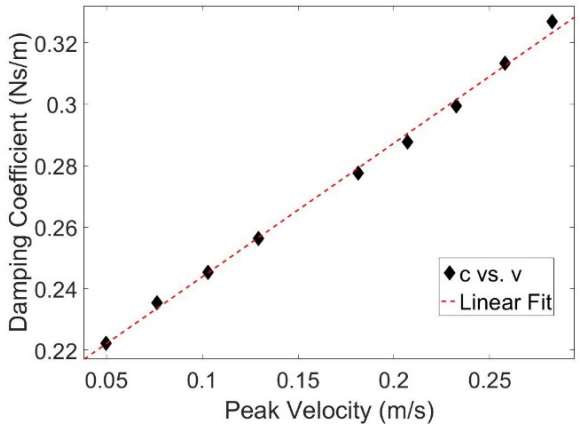

Figure 4. Linear fit of viscous damping coefficient versus peak velocity.

The clamps used to hold the leaf springs in place are the most likely source for this scaled energy dissipation. Losses can arise at the rubbing contact or through clamp elastic motion during vibration. Future tests will be completed to determine if the clamps are indeed the source for the variable viscous damping term. This will be done by designing and building two flexures with the same material and size: one monolithic and one with clamps.

FRICTION MODELS AND UNCERTAINTY

A single parameter Coulomb friction model was applied to determine the friction coefficient for the contact pair: a polytetrafluouroethylene (PTFE) pin on a polished steel counterface. To ensure a uniform interface between the polymer pin and steel counterface, a fine grit strip of sand paper was placed on the counterface and the polymer sample was run across it until its surface was parallel to the material plate. A normal force, *N*, of 14 N was applied for these tests.

Equation 2 was modified to include a friction force. The corresponding differential equation of motion is shown in Eq. 4, where the *m*, *k*, and *c* values were determined from free vibration tests with no friction contact. The friction force is $F_f = \mu N$, where μ is the friction coefficient and *N* is the normal force.

$$\begin{aligned} m\ddot{x} + c\dot{x} + kx + F_f &= 0, \dot{x} > 0 \\ m\ddot{x} + c\dot{x} + kx &= 0, \dot{x} = 0 \\ m\ddot{x} + c\dot{x} + kx - F_f &= 0, \dot{x} < 0 \end{aligned} \quad (4)$$

Due to the variations in the damping coefficient, two separate approaches were: 1) use the mean damping coefficient from the modal parameters; and 2) use the linear fit for the damping coefficient versus velocity.

For the former, a Monte Carlo simulation was completed to determine the propagation of uncertainties associated with each system parameter to the best fit on a single parameter friction model data set. This data set was artificially created to represent the perfect friction data set assuming a known Coulomb friction model. Each input variable was sampled 100,000 times from a normal distribution defined by the Table 2 standard deviations and its individual influence on the friction fitting equation of motion, Eq. 4, was determined. For the created data set the coefficient of friction, μ_d, was 0.15. Table 3 shows the results and Fig. 5 displays the probability density function for the case where all system parameter variables were randomly sampled in each iteration of the simulation. As expected, the highest uncertainty is associated with the damping coefficient. However, the highest sensitivity is presented by the modal mass.

Table 3. Monte Carlo simulation results.

μ_d			
Parameter	Mean	St. Dev.	dμ/dm (dk, dc)
m	0.150015	6.39×10^{-5}	1.31×10^{-2}
k	0.150018	2.09×10^{-5}	1.65×10^{-5}
c	0.150001	2.36×10^{-4}	6.93×10^{-3}
ALL	0.150021	2.48×10^{-4}	

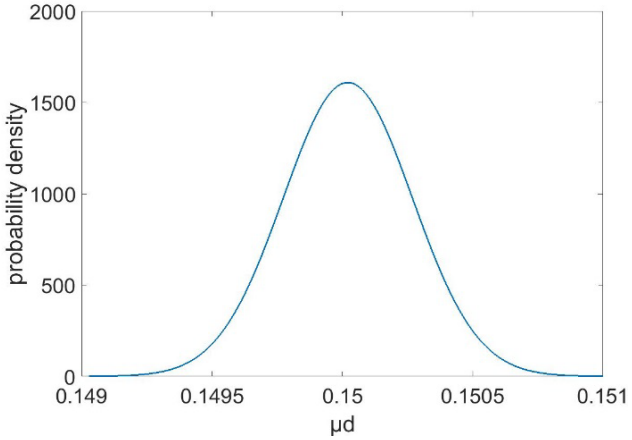

Figure 5. Probability density function for μ_d with m, k, and c variation.

In the second approach the linear relationship between viscous damping and velocity was applied. The fit is provided in Eq. 5.

$$c = 0.437\dot{x} + 0.2005 \quad (5)$$

Other potential damping models were tested as well, including Elliott and Tehrani's model [4] which implements a general nonlinear damping term for the analysis of a single degree of freedom system, Zaitsev's [5] model for nonlinear damping in doubly clamped beams, and a drag term to account for the flexure movement in air during oscillation. None provided a consistent result when applied to Eq. 2. Therefore, the simple viscous damping model was retained for friction fata fitting.

FRICTION FITTING RESULTS

The PTFE-polished steel contact pair was used to collect data sets at the same initial displacements as those that were used to establish the modal parameters. The repeatability of every initial displacement test was verified. Figure 6 shows five tests at the same initial displacement. It is observed that the measured velocity results are nearly identical.

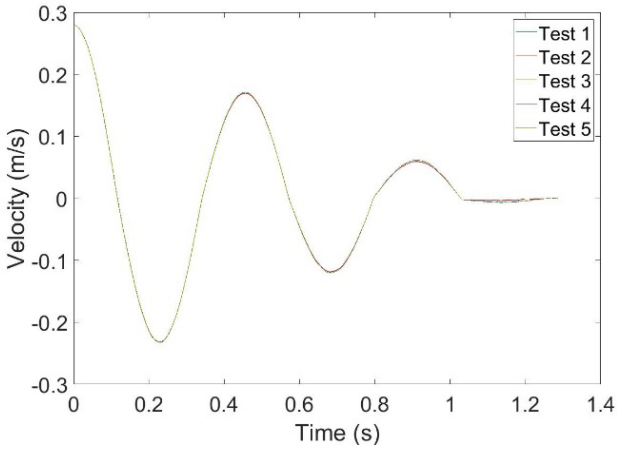

Figure 6. Vibrometer velocity data for five friction contact tests conducted at an initial displacement of 20 mm.

The friction fitting results for the mean and linear viscous damping approaches were similar. Table 4 shows the friction fitting results for initial displacements, x_0, ranging from {8 to 22} mm. Figure 7 displays a sample of the fitting for an initial displacement of 20 mm.

Table 4 Friction fitting results for various initial displacements, x_0.

	Linear c		Mean c	
x_0 (mm)	μ_d	v_{max} (m/s)	μ_d	v_{max} (m/s)
8	0.217	0.086	0.217	0.086
9	0.225	0.100	0.224	0.100
10	0.228	0.114	0.228	0.114
11	0.232	0.128	0.231	0.128
12	0.236	0.141	0.235	0.141
13	0.244	0.155	0.239	0.155
14	0.247	0.168	0.247	0.168
15	0.248	0.182	0.248	0.182
16	0.252	0.196	0.252	0.196
17	0.254	0.209	0.254	0.209
18	0.261	0.223	0.261	0.223
19	0.265	0.237	0.265	0.237
20	0.264	0.251	0.264	0.251
21	0.265	0.265	0.265	0.265
22	0.267	0.280	0.267	0.280

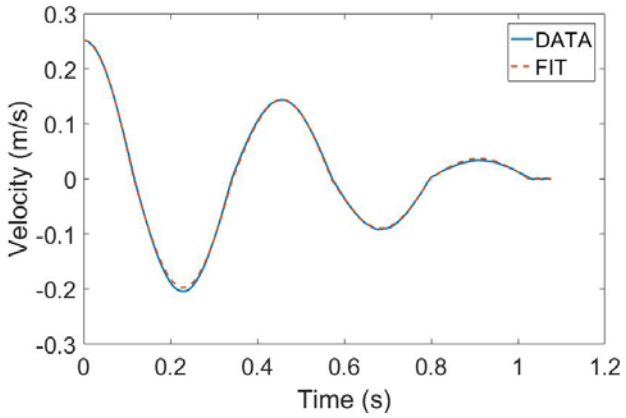

Figure 7. Friction fitting results using single parameter Coulomb friction model.

As with the viscous damping coefficient, the coefficient of friction displays a dependence on velocity as well. This is the case for both approaches, as can be seen in Fig. 8.

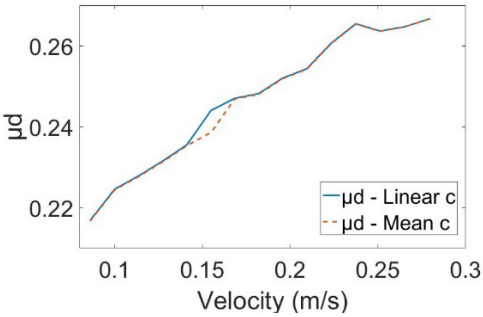

Figure 8. Friction coefficient versus velocity for both linear damping coefficient and mean damping coefficient approaches.

In this case, the relationship between μ_d and velocity can best be modeled through a power model; see Eq. 6. The Eq. 6 fit has an R^2 value of 0.99 and is visually presented in Fig. 9.

$$\mu_d = 0.311\dot{x}^{0.2116} + 0.03148 \qquad (6)$$

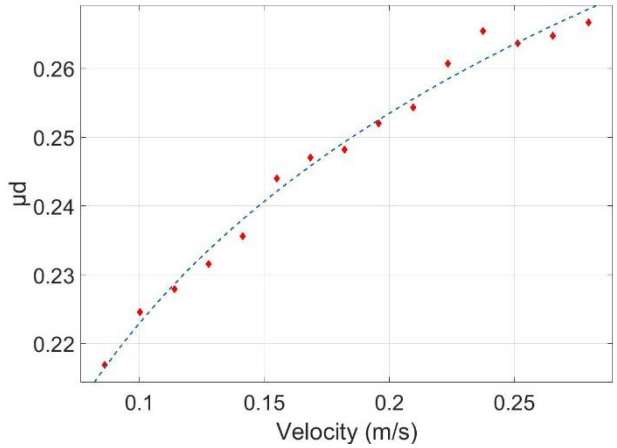

Figure 9. Power law fit for the μ_d versus velocity data.

The power law fit indicates that, at close to zero velocity, the friction coefficient is close to zero as well. As the velocity increases, so does energy dissipation. This behavior resembles the non-reversible friction model discussed by Wojewoda and Stefanski [6], where it is proposed that the sliding resistance due to friction is larger when an object accelerates from zero velocity than when is decelerates toward zero velocity. In both instances, the friction coefficient takes the same constant value once a specific velocity is reached.

The theory that the friction coefficient is larger or smaller depending on acceleration was tested in a separate simulation that considered the current acceleration at each time step of the Euler integration. This resulted in an improved fit to the data across the different initial displacement tests. The coefficient of friction was always found to be larger when the FMM was accelerating than when it was decelerating. Figure 10 displays these results and Eq. 7 displays the equation of motion.

$$\begin{aligned} m\ddot{x} + c\dot{x} + kx + \mu_{d1}N = 0 \quad ,\ddot{x} > 0 \\ m\ddot{x} + c\dot{x} + kx + \mu_{d2}N = 0 \quad ,\ddot{x} < 0 \end{aligned} \qquad (7)$$

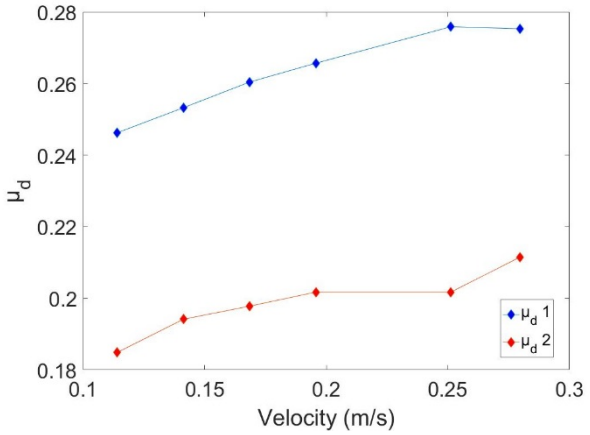

Figure 10. Dependence of the friction coefficient on acceleration (1 accelerating, 2 decelerating).

The final friction model for the data has yet to be determined. However, the ability to observe and measure the energy dissipation due to sliding friction velocity, rather than force, enables reduced uncertainty for this interrogation.

CONCLUSION

The goal of this research was to develop a new friction measuring method for low velocity, low friction applications. By using a laser vibrometer to measure velocity and using that data to determine energy dissipation due to friction, it is possible to achieve lower uncertainties when determining friction coefficients for sliding contact interfaces. The friction measuring machine (FMM) enables the relative contributions of structural and friction contact energy losses to be isolated and quantified. Once the system dynamics were established and the friction model was selected, it was possible to parameterize the sliding friction model.

REFERENCES

[1] Schmitz T, Action J, Ziegert J, and Sawyer WG (2005). On the Difficulty at Measuring Low Friction: Uncertainty Analysis for Friction Coefficient Measurements. Journal of Tribology 127: 673-678.

[2] Smith Stuart T (2000). Flexures: Elements of Elastic Mechanisms. CRC Press LLC, London UK.

[3] Schmitz T and Smith KS (2012). Mechanical Vibrations: Modeling and Measurement. Springer, New York, NY.

[4] Elliott, S.J. Tehrani, M.G. Langley, R.S (2015). Nonlinear damping and quasi-linear modelling. Royal Society Publishing.

[5] Zaitsev, S. Almog, R. Shtempluck, O. Buks, E. (2006) Nonlinear Damping in Nanomechanical Beam Oscillator. IEEE. 0-7695-2398-6.

[6] Wojewoda, J. Stefanski, A. Wiercigroch, M. Kapitaniak, T. (2008) Hysteretic effects of dry friction: modelling and experimental studies. Philosophical Transaction of the Royal Society, A.